Balmer-alpha emission and hydrogen-atom energy in ion-source discharges

D. H. McNeill
Plasma Physics Laboratory, Princeton University, P. O. Box 451, Princeton, New Jersey 08544

J. Kim
General Atomic Company, P. O. Box 81608, San Diego, California 92138
(Received 11 May 1981)

The structure of the hydrogen Balmer-alpha line emission profiles from three types of neutral-beam-injector ion-source plasmas [filling pressure ~ 10 mTorr, electron density $\sim(1-2)\times 10^{12}$ cm^{-3}, electron temperature $\sim 2-4$ eV] is studied with the aid of a simple model for the neutral-particle balance and H_α emission. This model includes molecular and atomic reactions, wall interactions, and nonthermal electrons. A large fraction of the H_α is produced by dissociative excitation of H_2 and dissociative recombination of H_2^+, while the remainder is produced by excitation of H atoms, most of which have energies that are close to the characteristic H_2 dissociation energies. The H_α linewidth is thus insensitive to the discharge operating conditions and equals ~ 0.27 Å when only slow (~ 0.3 eV) dissociatively excited atoms are present or ~ 0.35 Å when fast (> 1 eV) atoms, apparently also produced in dissociation reactions, are present as well.

I. INTRODUCTION

In this paper we present a qualitative account of discharge phenomena based on an interpretation of the Doppler-broadened profiles of hydrogen Balmer-alpha (H_α, 6563 Å) emission from some ion-source plasmas. Measurements of H_α light were made on three types of ion sources: a magnetic multipole line-cusp "bucket" source, a duopigatron ion source with a conventional oxide cathode, and the same duopigatron source with an incandescent tungsten thermal predissociator as a cathode. The data were obtained with a Fabry-Perot interferometer (FPI) whose high resolution made accurate analysis of the H_α profile shapes convenient. A model for the excitation of H_α in these discharges is developed in some detail. Wall recombination of H atoms, nonthermal fast electron populations, and various sources of H_α light and H atoms are taken into account. A clear distinction was found in some of the observed line profiles between light produced by dissociative excitation of molecules (and electron-impact excitation of atoms with energies close to the characteristic dissociation energies) and that produced by excitation of cold (wall temperature) background atoms.

Experiments in which electron beams with energies above about 15 eV bombard hydrogen gas and dissociate the H_2 molecules to yield excited hydrogen atoms in two groups with energies of roughly 0.3 and 3 eV have been reported extensively in the literature. However, we believe that this is the first time slow dissociation product atoms have been identified in a hydrogen discharge. The constancy of the H_α linewidth from each of the three ion sources is explained by the presence of these atoms. Our results on the H_α line profiles yielded information on other physical properties of the discharges, including the density and energy distribution of the neutral atom population and the possible occurrence of hot nonthermal electrons. This analysis should be of general interest in the spectroscopy of low-to-medium density hydrogen plasmas.

II. EXPERIMENT

A. The ion sources

The injection of high-energy neutral beams is the principal auxiliary heating scheme in large magnetically confined fusion experiments.[1] The largest neutral beam injectors in use today employ ion sources with discharge currents of 1 kA or more to produce hydrogen or deuterium ion currents of up to 100 A. These ion sources have a uniform discharge plasma over a large volume and the beams extracted from them contain a high fraction of atomic ions (H^+) compared with molecular ions

(H_2^+ and H_3^+). The partially ionized multicomponent plasmas in these ion sources are not well understood, to a great extent because of the large number of competing collision processes within the discharge volume and at the vessel walls.

The sources examined in these experiments were a 15-cm-diam line-cusp bucket (modified MacKenzie) source,[2] a 7-cm-diam duopigatron source with a conventional oxide cathode,[3] and the same 7-cm-diam duopigatron source with a hot tungsten predissociator as a cathode.[4] The diameters specified here refer to the diameters of the beams extracted from the sources (and to the approximate diameters of the discharge plasmas). We shall call these sources the bucket source, the conventional duopigatron source, and the modified duopigatron source, respectively.

The bucket source[2] consists of a cylindrical anode chamber with arrays of long bar magnets running parallel to its axis and forming a multiple-magnetic cusp, a number of tungsten filaments as a cathode, and an extraction structure consisting of three multiaperture grids with an extraction area of diameter 15 cm. The first grid (the "plasma grid") is in contact with the ion-source plasma and is at the cathode potential. In our experiments, the FPI viewed across the 25-cm-diam chamber through a 2.5-cm-diam port about 10 cm from the plasma grid. The arc discharge current was varied over 42–84 A and the arc voltage was about 80 V. The nominal flow-through filling pressure was 5–20 mTorr (slightly lower in the discharge volume).

The duopigatron ion source[3] consists of a cathode inside an intermediate electrode (connected to the positive side of the arc power supply through a 1-kΩ resistor), two anodes (No. 1 with a 0.03-Ω and No. 2 with a 0.01-Ω resistor to the positive side of the arc supply), and a 7-cm-diam plasma grid with multiple apertures (connected to the positive side of the arc supply through 200 Ω). The duopigatron discharge consists of two discharges separated by a double sheath near the intermediate electrode aperture: a glow discharge (duoplasmatron configuration) inside the intermediate electrode serves as a plasma feed for a Penning ion gauge (PIG) discharge in the extended-anode region with magnetic cusps. We observed the H_α light from the latter region a few cm above the plasma grid. Duopigatron discharges with two different types of cathode were examined: a conventional oxide filament[3] and an incandescent tungsten tube through which the supply gas is fed and and thereby thermally dissociated.[4] A hot tungsten tube has been used previously as a cathode and as a dissociator, together with thin tungsten sheet liners on the inside walls, in order to enhance the fraction of atomic ions in the discharge.[4] A somewhat wider range of filling pressures and arc currents was examined on the duopigatron sources than on the bucket source.

The plasma parameters for all three sources have the following measured values[2–4]: electron density $n_e=(1-2)\times 10^{12}$ cm^{-3}; electron temperature $T_e=2-4$ eV; and molecular density $n_{H_2}\sim 10^{14}$ cm^{-3}. The magnetic field in the bucket source is $\lesssim 100$ G at the edge of the discharge and <5 G in the central (10-cm-diam) region, while that in the duopigatron falls from about 200 G in the intermediate electrode region to about 20 G at the plasma grid. The plasma sizes are 7–20 cm, roughly equal to the extracted beam diameters, and the copper vacuum vessels have inside dimensions of 10–25 cm. The gas and plasma parameters may be regarded as reasonably uniform over the discharge. Certainly, n_e is uniform (that is one of the requirements for a large area source) and T_e is roughly so according to probe measurements. The densities of neutral molecules and atoms are close to uniform because their mean-free paths for loss by electron collisions are much greater than the vessel dimensions.[5] Charged-particle species measurements on the ion beams extracted from these sources indicate that the ion population in the discharge is close to 50% H^+, 30% H_2^+, and 20% H_3^+ ($n_e=n_{H^+}+n_{H_2^+}+n_{H_3^+}$).

B. The Fabry-Perot interferometer

A Burleigh Instruments RC-10 piezoelectrically scanning FPI was used as a spectrum analyzer. The interferometer consists of two partially transmitting mirrors (reflectivity 99% for wavelengths of 6000–7000 Å) mounted parallel to one another. When the FPI cavity is illuminated by a beam of collimated monochromatic light it will transmit the light if the optical distance between the reflecting surfaces is an integral number of wavelengths, i.e., the condition for constructive interference is satisfied.[6] The range of wavelengths that can be seen through the interferometer in the same order without overlapping into other orders is known as the free spectral range (FSR) and is given by $\Delta\lambda_{FSR}=\lambda^2/2d$, where d is the mirror separation and λ is the wavelength of the light (all dimensions

in the same units). The smallest obtainable width [full width half maximum (FWHM)] of the transmission peaks from the interferometer is called the minimum resolving bandwidth $\Delta\lambda_R$. The instrument function of the FPI is characterized by the finesse F, which is defined as $F=\Delta\lambda_{FSR}/\Delta\lambda_R$. The finesse is determined by numerous factors, including the reflectivity, flatness, and parallelism of the mirrors, the focal length and aperture of the collimating system, and mechanical vibrations. In our experiments the finesse was measured by using a helium-neon laser as a narrow linewidth source ($\lambda=6328$ Å with an overall linewidth of $\lesssim 0.02$ Å) and optimized by adjusting the mirrors to obtain maximum transmission of the laser beam. The distance between the mirrors and, therefore, the wavelength of peak transmission are varied periodically by applying a ramp voltage to piezoelectric transducers mounted on one of the mirror holders. The scan period, which includes from two to four interference orders, was varied between 20 and 200 msec, and the retrace lasted 15 msec. The rapid linear scan made it possible to observe the time variation of the light during a single arc pulse.

After passing through the FPI (5.0-cm-diam mirrors), the light from the plasma was focused by a collimating lens through a pinhole and onto a light guide. The light guide was directed through an intereference filter onto a photomultiplier tube. The interference filter blocked out background light from the plasma and the filaments. The photomuliplier output could be smoothed by an RC filter, but electrically unfiltered data were taken during each run to ensure that the RC filter did not distort the profiles.

C. Data

The top portion of Fig. 1 shows the location of the viewing port for observing the duopigatron ion source. (The lower portion shows the arrangement for optical studies of extracted neutral beams. They are the subject of a previous report.[7]) The optical system was aligned and the FPI tuned by passing a He-Ne laser through a viewing port located opposite the 1.25-cm-diam observation port and backwards along the optical train. No data were taken while the high-voltage beam-extraction system was operating.

Figure 2 shows oscilloscope traces of data from the conventional duopigatron discharge: (a) the arc current and the electrically unfiltered photomultiplier response to the H_α light from the plasma with three interference orders during the 200-msec arc pulse; (b) the RC filtered photomultiplier signal (triggered at the beginning of the arc) and a ten times magnified view of a single spike near the middle of the discharge; and, (c) the response of the entire optical system to a He-Ne laser beam and a ten times magnified trace of a single spike. In Fig. 2(c) the short and long scribe marks correspond, respectively, to the FWHM of the magnified spike and to the FSR of the interferometer at the laser wavelength. This shows that the finesse $F\sim 60$, so that the instrument resolution is $\Delta\lambda_R=0.035$ Å for the measured plate separation $d=0.10$ cm.

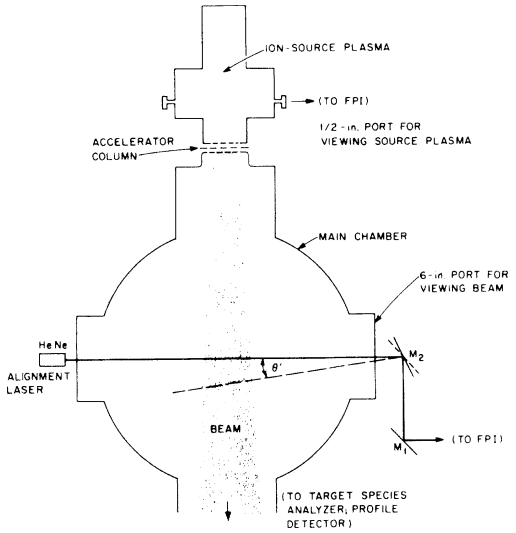

FIG. 1. A sketch of the duopigatron ion source and the beam chamber. The top portion shows the arrangement for FPI measurements on the 7-cm-diam source plasmas, and the bottom, that for observation (Ref. 7) of extracted beams.

The signal from the right-hand side of the expanded trace of Fig. 2(b) is plotted in Fig. 3 (curve A) as a function of the wavelength shift $\Delta\lambda$ (Å) from the profile peak. The bars indicate the range of signals obtained from a large number of discharges from this source under various operating conditions. The small bumps roughly 0.1 Å from the peak on both sides are a reproducible feature of all the H_α spectra taken on the conventional duopigatron source. This feature was not evident in the profiles from the bucket source, although it could have been lost in the noise. Except for the modified duopigatron source (see Fig. 4), all the plasmas yielded fairly symmetric H_α profiles with a FWHM of 0.27 ± 0.02 Å under all conditions and

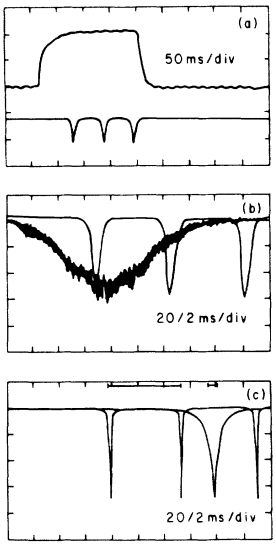

FIG. 2. FPI data from the 7-cm-diam duopigatron source with a conventional oxide cathode: (a) the arc current and unfiltered H_α photomultiplier output; (b) the filtered photomultiplier output with a 10× magnified trace of one spike; and, (c) the FPI response to a He-Ne laser, illustrating the resolution of the FPI.

at all times during the ≤ 200 msec discharges. Furthermore, these H_α profiles showed no discernible enhancement in the wings (to within 4% of the integrated line intensity) above a "Gaussian fit"

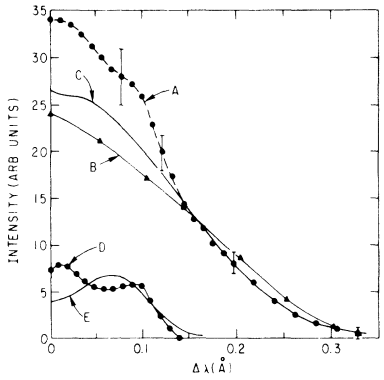

FIG. 3. (A) The signal from the right-hand side of the expanded trace of Fig. 2(b); (B) the H_α spectrum calculated from the kinetic-energy distribution of slow H(2s) dissociation product atoms (Ref. 12) normalized to curve A at 0.15 Å; (C) the H_α spectrum calculated for atoms with a temperature of 0.23 eV normalized to curve A at 0.14 Å; (D) the difference between curves A and C; (E) the H_α spectrum calculated for atoms with a temperature of 0.025 eV combined with a Gaussian instrument function of width 0.036 Å.

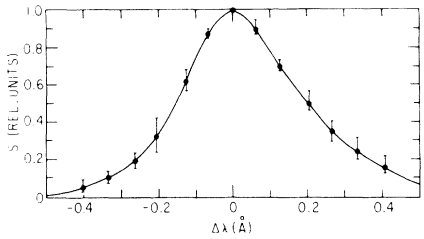

FIG. 4. The H_α spectrum obtained from the modified duopigatron source with a hot tungsten predissociator. The bars indicate the range of signals from a series of five discharges.

profile with the same half-width.

An asymmetric H_α spectrum with the long-wavelength side higher was observed on the modified duopigatron source. The plot in Fig. 4 was constructed from a series of five H_α traces from this source under various conditions. The discharge operating conditions (arc current and voltage, filling pressure) were the same as for the conventional duopigatron source. The intensity of the H_α light, however, is far higher in the wings ($\Delta\lambda \geq 0.3$ Å) than in the other cases. The line had approximately the same (within a factor of 2–3) total intensity as, and a larger FWHM (~ 0.35 Å) than, the profile of Fig. 3 (curve A).

III. H_α EMISSION PROCESSES IN LOW-TEMPERATURE DISCHARGES

A. Sources of H_α: Neutral particle energies

In these discharges several processes may produce excited hydrogen atoms (H*). We are concerned with excitation to the $n=3$ state and emission on the $n=3\rightarrow 2$ transition (H_α). The most probable excitation processes are: dissociative excitation or the formation of excited atoms during dissociation of H_2 molecules by electrons (cross section denoted by σ_{e2})[8]

$$e+H_2\rightarrow H^*+H+e\ ; \tag{1}$$

dissociative recombination of H_2^+ ions with electrons to yield an excited product atom ($k\sigma_{dr2}$, where $k<1$ is the fraction of the dissociative recombination reaction which yields a given state or line)[5,9]

$$e+H_2^+\rightarrow H^*+H\ ; \tag{2}$$

and, electron-impact excitation of H atoms (σ_{e1}),[10]

$$e+H \rightarrow H^*+e \ . \tag{3}$$

Radiative electron-ion recombination ($e+H^+ \rightarrow H^*$) is negligible.[11] It is not known whether excited atoms are produced during formation of H_3^+ in the reaction ($\sigma_{H_3^+}$) (Ref. 5)

$$H_2+H_2^+ \rightarrow H+H_3^+ \ , \tag{4}$$

the major process by which H_2^+ is lost in the ion source discharges and an important source of H atoms (product H atoms could be excited only if the H_3^+ is formed in an electronically excited state). We shall neglect it and the dissociation reactions of H_3^+ as sources of H_α under the assumption that the energy of H* from these reactions is similar to that from reactions (1) and (2) and because here we are primarily concerned with the qualitative distinction between H* produced in atomic [i.e., reaction (3)] and molecular processes. We also neglect the effect of vibrational excitation, or, more precisely, assume that the vibrational distributions of H_2 and H_2^+ in the discharge are similar to those in the original cross-section measurements.

Excited atoms formed by electron-impact dissociation of H_2 belong to one of two energy groups[12,13]: slow, with energies $E \sim 0.3$ eV (formed in states with $n \geq 2$ by electrons with energies $E_e \gtrsim 15$ eV) and fast, with energies $E \sim 2-8$ eV (formed by electrons with $E_e \gtrsim 28$ eV). The lower, 15 eV, threshold appears as a result of excitation of singly excited bound $(1s\sigma_g)(nl\lambda)$ states to energies above the dissociation energy. The higher threshold, which has some structure over $E_e \sim 23-45$ eV, is attributed to excitation of doubly excited repulsive $(2p\sigma_u)(nl\lambda)$ states. The sequence of transitions, including direct dissociation, predissociation, and level crossings, that follows the direct excitation of these states in the Franck-Condon region is the subject of extensive discussion in the literature (see, for example, Refs. 8, 12, and 13). In low-temperature plasmas with $T_e \lesssim 4$ eV, most dissociation product atoms will belong to the slow group because of the relatively small number of electrons with energies sufficient to produce fast excited atoms. The kinetic energies of the atoms produced in reactions of H_2^+ have not been measured, but H_α spectral profiles from tokamaks suggest that the kinetic energies of atoms formed in dissociative excitation of H_2^+ ($e+H_2^+ \rightarrow H^+ + H + e$) are similar to those formed in dissociative excitation of H_2.[14] Furthermore, from the potential-energy curves for H_2 and H_2^+, it is clear that most of the atoms formed by dissociative recombination of H_2^+ in low-temperature plasmas will belong to the slow group.

The mean-free path for elastic collisions between a newly formed 0.3-eV H atom and the cold (~ 0.025 eV) background neutrals (H and H_2) is ~ 2 cm.[15] The mean-free path for a ground state 0.3-eV atom to be excited by electron impact to the $n=3$ state in the ion-source plasmas exceeds 10^4 cm, which is much greater than the vessel size or the elastic collision mean-free path. Thus, unless they are completely absorbed at the walls, many of the H atoms that are eventually excited to the $n=3$ level will have lost energy in collisions with other gas particles and the walls. The H_α transition occurs much more rapidly than any other collision process (the emission mean-free path is <1 mm). Therefore, the H_α produced by dissociation of H_2 or H_2^+ will come from emitting atoms with the characteristic dissociation energies (~ 0.3 or ~ 3 eV), while that produced by excitation of ground-state H atoms will come from emitters that have a spread of energies ranging from the dissociation energy to the thermal energy of the neutral gas in the vacuum vessel. We shall distinguish these three sources of H_α and call them, respectively, slow molecular H_α, fast molecular H_α, and atomic H_α.

B. Model for neutral particle balance and H_α production

In order to analyze the production of H_α light, we begin with an estimate of the relative populations of atoms and molecules in the ion-source discharges ($T_e = 2-4$ eV, $n_e = 10^{12}$ cm^{-3}, $n_{H_2} = 10^{14}$ cm^{-3}, and $n_{H^+}:n_{H_2^+}:n_{H_3^+} = 50:30:20$). The following reactions produce most of the H atoms in moderate-density thermal discharges with $T_e \leq 4$ eV:[5] dissociation of H_2 (σ_d)

$$e+H_2 \rightarrow H+H+e \ ; \tag{5}$$

dissociative recombination of H_2^+ (σ_{dr2})

$$e+H_2^+ \rightarrow H+H \ ; \tag{6}$$

H_3^+ formation ($\sigma_{H_3^+}$), reaction (4); and, dissociative recombination of H_3^+ (σ_{dr3})

$$e+H_3^+ \rightarrow H+H+H \ . \tag{7}$$

In these discharges almost all the H_2^+, formed by electron-impact ionization of H_2 (σ_{ion})

$$e+H_2 \rightarrow H_2^+ + 2e \ , \tag{8}$$

is lost inside the plasma before it reaches the walls since the time for loss in reactions (4) and (6) is much shorter than the time for H_2^+ to reach the walls from the center of the discharge. Furthermore, most of the H_2^+ will yield H atoms, rather than protons,[5] either directly [reactions (4) and (6)] or indirectly [reaction (4) followed by reaction (7)]. Therefore, the rate of production of H atoms in the discharge is given approximately by twice the sum of the rates of dissociation and ionization of H_2:

$$2n_e n_{H_2}(\langle\sigma_d v_e\rangle+\langle\sigma_{\rm ion}v_e\rangle)\ \text{atoms/cm}^3\text{s}\ , \quad (9)$$

where $\langle\sigma_x v\rangle$ denotes the rate coefficient for reaction x.

Following Gabovich's treatment[16] of the particle balance in ion sources, we equate the rate of production of H atoms to the rate of recombination of H at the walls:

$$2n_e n_{H_2}(\langle\sigma_d v_e\rangle+\langle\sigma_{\rm ion}v_e\rangle)V=\tfrac{1}{4}n_H\bar{v}_H\gamma S\ , \quad (10)$$

where V is the volume of the plasma, S is the surface area of the vacuum vessel, $\bar{v}_H$ is the mean velocity of the hydrogen atoms in the discharge (2.5×10^5 cm/s for the wall temperature of $\sim$290 K and 7×10^5 cm/s for the most probable dissociation energy), and γ is the fraction of neutral atoms incident on the wall that undergo recombination to form molecules (more precisely, here γ represents the sticking probability for H atoms). Here we assume that all ions recombine at the walls to form molecules and that the plasma parameters are uniform. In the case of a sphere of radius R (chosen for simplicity of analysis) filled with plasma, this yields

$$\frac{n_H}{n_{H_2}}=\frac{8Rn_e(\langle\sigma_d v_e\rangle+\langle\sigma_{\rm ion}v_e\rangle)}{3\gamma\bar{v}_H}\ , \quad (11)$$

for the ratio of atom and molecule densities in the plasma. (Here it is assumed that $n_{H_2}>>n_H$, but the modification for high degrees of dissociation follows immediately from conservation of the number of atoms.)

The ratio of the atomic H_α emissivity ϵ_a (reaction 3) to the molecular H_α emissivity ϵ_m (reactions 1 and 2) is given by[9]

$$\frac{\epsilon_a}{\epsilon_m}=\frac{n_e n_H\langle\sigma_{e1}v_e\rangle}{n_e n_{H_2}\langle\sigma_{e2}v_e\rangle+0.044n_e n_{H_2^+}\langle\sigma_{dr2}v_e\rangle}$$

$$=\frac{n_H\langle\sigma_{e1}v_e\rangle}{n_{H_2}\langle\sigma_{em}v_e\rangle}\ . \quad (12)$$

Here[17]

$$\langle\sigma_{em}v_e\rangle=\langle\sigma_{e2}v_e\rangle+0.044\frac{n_{H_2^+}}{n_{H_2}}\langle\sigma_{dr2}v_e\rangle$$

$$\approx\langle\sigma_{e2}v_e\rangle+\frac{n_e}{n_{H_2}}\langle\sigma_{\rm ion}v_e\rangle \quad (13)$$

is an effective cross section for H_α emission from molecular dissociation that includes the formation of H_2^+ from H_2 ($\langle\sigma_{dr2}v_e\rangle\sim3\times10^{-8}$ cm^3/s for $T_e=2-4$ eV).[5] Hence, for a sphere of radius R

$$\frac{\epsilon_a}{\epsilon_m}=\frac{8Rn_e(\langle\sigma_d v_e\rangle+\langle\sigma_{\rm ion}v_e\rangle)\langle\sigma_{e1}v_e\rangle}{3\gamma\bar{v}_H\langle\sigma_{em}v_e\rangle}\ . \quad (14)$$

We note that the two contributions to $\langle\sigma_{em}v_e\rangle$ are roughly equal and that in Eq. (9) the second part contributes less than 20% over the entire temperature range of interest.[5,8,9]

Equations (11) and (14) have a reciprocal dependence on the surface recombination coefficient γ. With copper, Wood and Wise measured $\gamma\lesssim0.14$ for a filament probe and $\gamma=0.19$ for an evaporated film.[18] The copper walls of the ion sources are probably coated with contaminants, are rough on a microscopic scale, and do not qualify as high-purity materials. Thus, it is difficult to specify a precise value of γ, but it is probably higher than these values. A qualitative theoretical discussion by Ali-Khan *et al.*,[19] indicates that the sticking probability at metal surfaces for H atoms with energies below a few tenths of an electron volt approaches unity. Evidently, the larger γ is, the smaller the number of H atoms in the discharge and the greater the relative amount of molecular H_α. γ and $\bar{v}_H$ are related in these plasmas. This can be seen qualitatively as follows. At low pressures, for $\gamma\sim1$, the H atoms will experience few collisions with background gas particles before being lost at the walls, so that the H atoms in the gas will have energies close to the characteristic dissociation energy, 0.3 eV. Conversely, if $\gamma<<1$, the atoms will be slowed down both at the walls and in gas-phase collisions, so the kinetic energy of most of them will approach the background gas temperature and n_H will become very large [cf. Eq. (11)]. Since $\gamma\sim0.2$, we may expect the atoms to have an "intermediate" nonthermal energy distribution.

In accordance with this discussion of the surface recombination coefficient, let us assume that the atoms in the plasma belong to two groups, hot and cold, with energies of approximately 0.3 and 0.025

eV, respectively (we may then write $n_H = n_{H\,hot} + n_{H\,cold}$). In the spectral data for the duopigatron source (see Sec. IV A), because of its narrow Doppler width the cold atom H_α can be isolated from the remainder of the H_α profile (which is roughly half molecular H_α). Thus, the observations provide a lower limit to the ratio of the intensity of emission from the cold H atoms (ϵ_{ac}) to the molecular emission, ϵ_{ac}/ϵ_m (ϵ_{ah}, the emissivity from hot H atoms cannot be separated optically from ϵ_m). As we shall see, this estimate provides a starting point for determining the populations of the two groups of atoms. The ratio ϵ_{ac}/ϵ_m is evidently also given by $\epsilon_{ac}/\epsilon_m = [n_e n_{H\,cold}\langle\sigma_{e1}v_e\rangle]/[n_e n_{H_2}\langle\sigma_{em}v_e\rangle]$. Hence, for known T_e and n_{H_2}, we have

$$n_{H\,cold} = \left[\frac{\epsilon_{ac}}{\epsilon_m}\right] n_{H_2} \frac{\langle\sigma_{em}v_e\rangle}{\langle\sigma_{e1}v_e\rangle} . \tag{15}$$

An analogous expression exists for $n_{H\,hot}$ ($\epsilon_{ac} \to \epsilon_{ah}$).

If a monoenergetic group of hot nonthermal electrons constitutes a fraction η of the total electron population, then the effect of such a group can be included in Eqs. (11) and (14) by replacing the rates $\langle\sigma v_e\rangle$ by $(1-\eta)\langle\sigma v_e\rangle + \eta\sigma_f v_f$, where σ_f is the cross section for an electron with energy E_f and v_f is the velocity of an electron with energy E_f. In an ion source, the primary electrons emitted from the cathode are accelerated across the cathode fall (cathode-anode potential $\gtrsim 80$ eV). A fraction of these electrons may reach the observation volume without having lost all their energy in collisions, although this has not previously been confirmed experimentally in these ion sources.

The fraction ϵ_{mF}/ϵ_m of the molecular H_α emissivity (ϵ_m) in the fast molecular component (ϵ_{mF}) is very sensitive to the presence of fast electrons in a low-temperature plasma. For $E_e > 28$ eV, roughly equal amounts of the dissociatively excited $H(n=3)$ atoms are in the fast and slow groups, while for $16 < E_e < 28$ eV, they are all in the slow group.[13] If a small nonthermal group with $E_f < 28$ eV is present it will slightly reduce ϵ_{mF}/ϵ_m, while if $E_f > 28$ eV the effect may be calculated as follows:

$$\frac{\epsilon_{mF}}{\epsilon_m} \cong \frac{1}{2}\frac{\eta\sigma_{emf}v_f + (1-\eta)\sigma_{em}(28)v_e(28)\Phi(28,T_e)}{n\sigma_{emf}v_f + (1-\eta)\langle\sigma_{em}v_e\rangle} . \tag{16}$$

Here $\Phi(E,T_e) \sim 1.1(E/T_e)^{1/2}\exp(-E/T_e)$ is the fraction of an electron population at temperature T_e with kinetic energy above $E(>>kT_e)$, σ_{emf} denotes the cross section for molecular H_α emission for an electron energy of E_f [the appropriate generalization of Eq. (13) must include dissociative excitation of $H_2^+, e + H_2^+ \to H^+ + H + e$ at high electron energies[5]], and $\sigma_{em}(28)$ and $v_e(28)$ denote the quantities for $E_e = 28$ eV [the onset energy for fast $H(n=3)$]. While this expression is extremely sensitive to the presence of a small group of nonthermal hot electrons, ϵ_a/ϵ_m and n_H/n_{H_2} are comparatively insensitive. The effect of nonthermal electrons is more pronounced for low T_e plasmas because the fraction of fast electrons in the Maxwellian distribution is small.

C. Results of the model for the duopigatron source

Table I lists some sample calculations for the duopigatron source using the expressions derived in the preceding section. The radius of the ion-source plasma is $R \sim 3.5$ cm, $n_e = 10^{12}$ cm^{-3}, and $n_{H_2} \sim 10^{14}$ cm^{-3}. As mentioned previously, a major difficulty in the use of this model is the lack of reliable data on γ and $\bar{v}_H$. Later, in interpreting our data, we shall consider two cases: (a) $\gamma \sim 1$ with $\bar{v}_H = 7\times10^5$ cm/s, and (b) $\gamma = 0.2-0.3$ with $\bar{v}_H = 4\text{-}5\times10^5$ cm/s (i.e., $\gamma\bar{v}_H = 1-7\times10^5$ cm/s). The table lists the following quantities for thermal plasmas with $T_e = 2$, 3, and 4 eV in the absence of fast electrons ($\eta = 0$) and in the presence of 2% and 5% groups of monoenergetic electrons with energies $E_f = 25$ and 40 eV: n_H/n_{H_2} from Eq. (11); ϵ_a/ϵ_m from Eq. (14); $n_{H\,cold}\, n_{H_2}^{-1}(\epsilon_{ac}/\epsilon_m)^{-1}$ from Eq. (15); and, ϵ_{mF}/ϵ_m from Eq. (16) for $E_f = 40$ eV (which is above the threshold for production of fast excited atoms in the dissociative excitation of H_2) and from a similar equation for $E_f = 25$ eV (below the threshold). The estimated errors in the calculations are $\lesssim 40\%$ based on the accuracy of the cross-section measurements.

From the calculations given in the table we can notice a number of effects: (i) As T_e becomes higher, n_H/n_{H_2} increases, and, thus, the relative amount of atomic H_α emission (ϵ_a/ϵ_m) rises as

TABLE I. Calculated values of the ratios of the atom density to the molecule density (n_H/n_{H_2}) and of the atomic H_α emissivity to the molecular H_α emissivity (ϵ_a/ϵ_m), of the cold (wall temperature) atom density ($n_{H\,cold}$), and of the fraction of molecular H_α produced by fast dissociation product atoms (ϵ_{mF}/ϵ_m) for a duopigatron plasma with $R=3.5$ cm, $n_e=1\times10^{12}$ cm^{-3}, and $n_{H_2}\sim10^{14}$ cm^{-3} for fast-electron fractions $\eta=0$, 0.02, and 0.05 and fast electron energies $E_f=25$ and 40 eV. The expected value of $\gamma\bar{v}_H$ is in the range $(1-7)\times10^5$ cm/s.

		$\eta=0.02$		$\eta=0.05$	
$T_e=2$ eV	$\eta=0$	$E_f=25$ eV	40 eV	$E_f=25$ eV	40 eV
$n_H/n_{H_2}\times\gamma\bar{v}_H$	2.4×10^3	9.5×10^3	1.2×10^4	2.0×10^4	2.4×10^4
$\epsilon_a/\epsilon_m\times\gamma\bar{v}_H$	6.5×10^4	6.2×10^4	5×10^4	1.2×10^5	1.0×10^5
$n_{H\,cold}n_{H_2}^{-1}(\epsilon_m/\epsilon_{ac})$	0.04	0.15	0.23	0.17	0.25
ϵ_{mF}/ϵ_m	2×10^{-3}	8×10^{-5}	0.48	4×10^{-5}	0.50
$T_e=3$ eV					
$n_H/n_{H_2}\times\gamma\bar{v}_H$	1.0×10^4	1.7×10^4	1.9×10^4	2.7×10^4	3.2×10^4
$\epsilon_a/\epsilon_m\times\gamma\bar{v}_H$	1.1×10^5	1.4×10^5	1.2×10^5	1.9×10^5	1.5×10^5
$n_{H\,cold}n_{H_2}^{-1}(\epsilon_m/\epsilon_{ac})$	0.09	0.12	0.17	0.14	0.21
ϵ_{mF}/ϵ_m	1×10^{-2}	4×10^{-3}	0.36	2×10^{-3}	0.43
$T_e=4$ eV					
$n_H/n_{H_2}\times\gamma\bar{v}_H$	2.7×10^4	3.5×10^4	3.5×10^4	4.5×10^4	5×10^4
$\epsilon_a/\epsilon_m\times\gamma\bar{v}_H$	2.5×10^5	3.0×10^5	2.7×10^5	3.2×10^5	2.7×10^5
$n_{H\,cold}n_{H_2}^{-1}(\epsilon_m/\epsilon_{ac})$	0.11	0.12	0.14	0.13	0.18
ϵ_{mF}/ϵ_m	3×10^{-2}	2×10^{-2}	0.22	1×10^{-2}	0.32

well. (ii) The fraction of fast molecular H_α (ϵ_{mF}/ϵ_m) increases with T_e for $E_F<28$ eV. (iii) The extreme sensitivity of ϵ_{mF}/ϵ_m to the presence of a hot-electron component with $E_f>28$ eV is evident in the table. A separate calculation shows that for $E_f=40$ eV, $\epsilon_{mF}/\epsilon_m\geq0.1$ for $\eta\geq0.005$ when $T_e\leq4$ eV. The presence of a hot-electron component with $E_f<28$ eV, on the other hand, reduces the relative amount of emission from the fast dissociation products for fixed T_e. (iv) The amount of atomic H_α relative to molecular H_α, ϵ_a/ϵ_m, exhibits a (weak) minimum at some fraction $\eta=\eta_{min}$. This ratio, however, is comparatively insensitive to T_e when T_e is 3 eV or more. (v) One may expect to see substantial amounts of molecular H_α compared to atomic H_α in ion-source discharges of this type for fixed n_e with combinations of the following characteristics: low bulk T_e, large wall recombination (sticking) coefficients, and very low pressures. Other molecular reactions besides reactions (1) and (2) may, of course, add to the molecular H_α contribution.

IV. INTERPRETATION OF THE SPECTRAL DATA

A. Doppler broadening

The principal cause of the H_α broadening observed in our experiments is Doppler broadening. Other effects are relatively small[20]: the instrument width was 0.035 Å in the data of Fig. 3 (curve A), and Stark broadening and Zeeman splitting cannot exceed 0.02 and 0.01 Å, respectively. The measured H_α linewidth was found to be constant at 0.27 ± 0.02 Å for the bucket and conventional duopigatron sources under all operating conditions. (We defer discussion of the modified duopigatron and its wider H_α profile until the end of the next section.) This suggests that the width is determined principally by molecular processes which yield atoms of fixed energies. Emitting atoms with an isotropic kinetic energy distribution $f_E(E)$ yield a Doppler broadened spectral profile whose shape $I(\Delta\lambda)$ is given by

$$I(\Delta\lambda) \propto \int_{E(\Delta\lambda)}^{\infty} E^{-1/2} f_E(E)\, dE \ , \qquad (17)$$

where $E(\Delta\lambda)=mc^2\Delta\lambda^2/(2\lambda_0^2)$, $\Delta\lambda$ is the wavelength shift relative to the proper wavelength λ_0, m is the mass of an atom, and c is the speed of light. Hydrogen atoms with a temperature T_H (eV) have Doppler-broadened 6563-Å H_α fine-structure components with a Gaussian shape of FWHM $0.504T_H^{1/2}$ (Å). The kinetic-energy distributions of both the fast and slow dissocation product atoms from H_2, however, differ somewhat from Maxwellian.[12] In particular, the slow group is deficient at both high and low energies compared to a Maxwellian energy distribution having the same most probable energy.

Ideally, Eq. (17) should be inverted to yield the H atom energy distribution from our data. However, given the mathematical difficulty of doing this when precise fine-structure information is lacking and the initial data are so noisy, we have chosen the simpler procedure of comparing our observations with calculated profiles based on available data about the kinetic-energy distribution of dissociation product atoms. Figure 3 shows: (A) the measured H_α profile from the conventional duopigatron source; (B) a calculated H_α spectrum using Eq. (17) for the case of two equally intense (as the observed profile A is symmetric) fine-structure components located 0.14 Å apart[21] for atoms having the energy distribution of slow dissociation product H(2s) atoms measured by Misakian and Zorn[12]; (C) as curve B except for Maxwellian atoms with temperature $T_H=0.23$ eV; (D) the difference between curves A and C; and, (E) the calculated H_α spectrum for Maxwellian atoms with $T_H=0.025$ eV and relative fine structure intensities of 1, 0.3, and 1 at $\Delta\lambda=-0.07$, 0, and 0.07 Å, respectively, combined with a Gaussian[22] instrument function with an FWHM of 0.036 Å. Curves C and B are normalized to curve A at $\Delta\lambda=0.14$ and 0.15 Å, respectively. Misakian and Zorn, and Ryan *et al.*,[12] have used time-of-flight energy resolution to measure the kinetic-energy distribution of H(2s) atoms produced by electron-beam dissociation of H_2 gas. Numerous measurements of beam-excited dissociative excitation Balmer line profiles have been made recently, but none yield kinetic-energy distributions[23] with as good resolution as the time-of-flight data for H(2s). The spectral data of Ref. 13 show that the average energies of excited atoms in states 3–6 are about the same as those in $n=2$. Assuming that the kinetic-energy distribution of H*($n=3$) is the same as that of H(2s) and given the much greater accuracy of the time-of-flight data, we have used the kinetic-energy distribution for H(2s) in our profile calculations. Considering the rather large errors in Misakian and Zorn's measurements at low energies[12] (i.e., in curve B for $\Delta\lambda<0.1$ Å), one can approximate the H_α spectrum (B) from the slow dissociation product atoms rather well by curve C, which is based on a Maxwellian distribution of atoms. For $\Delta\lambda>0.15$ Å, curves A, B, and C are in good agreement.

B. Energies of H atoms and fast nonthermal electrons in the discharges

The measured H_α linewidth of 0.27 ± 0.02 Å is slightly less than that reported in spectroscopic observations of the slow excited H($n=3$) atoms formed during dissociative excitation of hydrogen gas by an electron beam,[13] which was 0.31 Å (when the fine-structure correction is recombined with the derived Doppler width). Our experimental H_α profile (curve A of Fig. 3) is also somewhat narrower than that (curve B) derived for the measured H(2s) kinetic-energy distribution. The small symmetric bumps at $\Delta\lambda\approx\pm0.1$ Å in the traces from the duopigatron source appear to be a consequence of H_α emission from cold background atoms which have been excited by electron impact. Thus, as shown in Fig. 3, the measured H_α spectrum is the sum of contributions from slow dissociation product atoms (plus some amount from "re-excitation" of fresh dissociation product atoms that have not been slowed down, i.e., from $n_{H\,hot}$, that is indistinguishable in terms of its Doppler width from the slow molecular H_α) and from thermalized background atoms; that is, curve A is the sum of curves C ($\approx$ curve B) and D. The closeness [in terms of the profile width and to the extent that the noise level (see Fig. 2) is comparable to the difference between profiles D and E] of the calculated spectrum (E) for thermal atoms with $T_0=0.025$ eV (290 K) to curve D supports this division of the emitting-atom population into hot and cold groups ($\sim$0.3 and 0.025 eV). This part (D) of the spectrum produces the small bumps at $\Delta\lambda\sim\pm0.1$ Å and causes a slight narrowing of the spectrum compared to that obtained for dissociative excitation alone (curve B). Narrowing may also occur because some of the atoms that are "re-excited" will have lost energy, but not enough to "put" them in the cold atom group. (The difference between curves A and B for $\Delta\lambda>0.15$ Å sug-

gests this, but the experimental errors in both preclude a firm conclusion.)

The area under curve C is roughly five times that under curve D; thus, $\epsilon_{ac}/\epsilon_m \geq 0.2$. For thermal plasmas with $T_e = 2$, 3, and 4 eV, Eq. (15) shows that $n_{\mathrm{H\,cold}} \geq 0.8$, 1.8, and 2.2×10^{12} cm^{-3}, respectively ($n_{\mathrm{H}_2} = 10^{14}$ cm^{-3}). From the table it is clear that model case (a) ($\lambda\bar{\nu}_{\mathrm{H}} = 7\times10^5$ cm/s), besides implying that there should be no cold atoms, yields a value of n_{H} that is below these values of $n_{\mathrm{H\,cold}}$ for $T_e < 4$ eV in a thermal plasma. We thus choose, still somewhat arbitrarily, case (b) ($\gamma\bar{\nu}_{\mathrm{H}} = 1\times10^5$ cm/s) to obtain a crude estimate of the atom density and energy distribution, and we use the probe data and beam-species measurements to set $T_e = 3$ or 4 eV. According to the table, a fast electron component that constitutes at most a few percent of an electron population with $T_e \geq 3$ eV has little effect on $n_{\mathrm{H}}/n_{\mathrm{H}_2}$ or ϵ_a/ϵ_m. Thus, for $n_{\mathrm{H}_2} = 10^{14}$ cm^{-3}, we have $n_{\mathrm{H}} = (1.0-2.7)\times10^{13}$ cm^{-3} (corresponding to $T_e = 3-4$ eV). The corresponding $\epsilon_a/\epsilon_m = 1.1-2.5$, so that approximately 57–35 % of the intensity under curve C of Fig. 3 is molecular H_α and the rest is hot ($\sim$0.3 eV) atomic H_α. The actual value of ϵ_{ac}/ϵ_m is thus about 0.4 (0.35–0.57), so that $n_{\mathrm{H\,cold}} \gtrsim 4\times10^{12}$ cm^{-3}, while $n_{\mathrm{H\,hot}} \sim (0.6-2)\times10^{13}$ cm^{-3}. This qualitative relationship will hold for other reasonble choices of $\gamma\bar{\nu}_{\mathrm{H}}$. It therefore appears (despite the lack of precise data on the surface recombination coefficient) that hot ($E \sim 0.3$ eV) atoms are more numerous than cold ($\sim$0.025 eV) in the duopigatron ion source; i.e., most atoms are not slowed down to the background (wall) temperature before they are lost. The relative amounts of hot and cold atoms are independent of n_{H_2} at the typical operating pressures. Since the bucket source also yields H_α profiles that are slightly narrower than those obtained from molecular H_α alone, atomic H_α is probably superimposed on the molecular H_α in this discharge as well. The bumps corresponding to cold atomic H_α may be lost in the noise because of a smaller cold atom population or because the background gas may be warmer.

In the modified duopigatron source the operating conditions were the same as in the conventional one, but the H_α spectrum obtained from it (Fig. 4) was strikingly different (cf. Fig. 3, curve A). Since this profile extends beyond $\Delta\lambda = 0.4$ Å, it is clear that atoms with velocities in excess of 1.8×10^6 cm/s ($E > 1.5$ eV) exist in this plasma. The asymmetry of this profile, unlike that of Fig. 3 (cf. Ref. 22), is consistent with the relative fine-structure intensities reported in Ref. 21. The H_α spectra from the modified source can be resolved into two components of similar intensity: one with a width close to that observed in the conventional duopigatron (slow molecular + "hot," 0.3 eV, atomic H_α) and the other with a width $\gtrsim$0.7 Å (produced by emitting atoms with energies over 1 eV). The second component is not as wide as the fast molecular H_α spectrum observed in electron-beam bombardment of H_2 gas,[13] presumably because a significant portion of this component of the ion-source profile is produced by excitation of fast dissociation product atoms that have been slowed down in repeated collisions with the walls[24] and the background gas. There are two possible mechanisms by which atoms with energies above 1.5 eV may appear in the discharge. The first involves Coulomb collisional heating of H_2^+ ions by H^+ in the discharge to temperatures on the order of 1–2 eV, followed by dissociation of the hot H_2^+ by low-temperature electrons. (The H_2, unheated, would provide the narrower H_α component.) However, since the known plasma parameters (n_e, T_e) are the same as in the conventional source, there is little reason to expect the H^+ to be significantly hotter than in the modified source. (This mechanism could be important in a plasma with the required T_{H^+} and a much lower n_{H_2}.) The second mechanism is for a small population of fast electrons with energies above the threshold for production of fast dissociation product atoms to enhance the fast molecular H_α intensity (see the Table).[25] A fraction $\eta \gtrsim 0.005$ is sufficient to produce the effect observed here. (A small difference in the energy distributions of the hot nonthermal-electron populations in the two sources would cause no noticeable difference in the other plasma parameters.) The appearance of a slightly hotter electron population in the modified source might be a result of some change induced by the additional dissociation and heating of H_2 by the hot tungsten (e.g., a pressure change) or simply a result of geometrical changes inside the intermediate electrode which permit hotter electrons to move deeper into the PIG region (e.g., greater length of the cathode). The modified duopigatron results are of particular interest because, despite the obvious immediate differences in the H_α spectrum, they appear to confirm our earlier conclusions about the mechanisms by which H_α light and H atoms are produced and about the magnitude of the surface recombination (sticking) coefficient.

V. CONCLUSION

A model for the production of H_α in discharges with $T_e = 2-4$ eV, $n_e = (1-2)\times 10^{12}$ cm^{-3}, and $n_{H_2} \sim 10^{14}$ cm^{-3} has been used to interpret the H_α line emission from three types of neutral-beam-injector ion sources. The relative amounts of H_α emission from the slow ($E \sim 0.3$ eV) and fast ($E \sim 3$ eV) atoms formed by electron-impact dissociative excitation of H_2 and dissociative recombination of H_2^+ and from the electron-impact excitation of cold (~ 290 K) and hot (~ 0.3 eV) background H atoms have been calculated for a duopigatron source. A rough analysis of the data from the conventional duopigatron source shows that $n_H = (1-2.5)\times 10^{13}$ cm^{-3}, of which about 4×10^{12} cm^{-3} are at the wall temperature and $(6-20)\times 10^{12}$ cm^{-3} are at energies close to the slow dissociation product energy (0.3 eV). 25–45 % of the total intensity of the H_α light from the plasma is produced by electron-impact dissociation of H_2 and H_2^+ (this fraction may be greater if other reactions of H_2^+ and H_3^+ yield H_α). The H_α spectral profile is sensitive to the presence of fast nonthermal electrons and to the energy dependence of the surface recombination (sticking) coefficient for H atoms. In the conventional duopigatron and in the bucket source, all the H_α emission appears to come from slow dissociation product atoms (some are slowed down), while in the modified duopigatron source a substantial fraction of the emitting atoms have energies above 1 eV. These atoms seem to be fast product atoms from the dissociation of H_2 and they are probably created by a small population (0.5% of the total electron density is sufficient) of nonthermal electrons with energies in excess of the threshold for production of fast dissociation product atoms.

We have demonstrated the importance of molecular processes in the H_α spectrum and neutral particle balance for a series of ion-source plasmas. This interpretation should, with appropriate modifications, be widely useful in the spectroscopy of low-to-medium density hydrogen plasmas. A similar resolution of the H_α spectrum into two components, which appear to correspond to slow and fast molecular dissocation products, has been observed in several plasmas, including the microwave heated Elmo bumpy torus[26] and the edge region of tokamaks.[14]

ACKNOWLEDGMENTS

This work was supported by the U. S. Department of Energy under contracts No. DE-AC02-76-CHO3073 (D. H. M.) and DE-AT03-76-ET51011 (J. K.). We would like to thank our Oak Ridge colleagues R. C. Davis, P. M. Ryan, and C. C. Tsai for help in conducting the experiments.

[1] L. R. Grisham, Science 207, 1301 (1980).
[2] W. L. Stirling, P. M. Ryan, C. C. Tsai, and K. N. Leung, Rev. Sci. Instrum. 50, 102 (1979).
[3] R. C. Davis, T. C. Jernigan, O. B. Morgan, L. D. Stewart, and W. L. Stirling, Rev. Sci. Instrum. 46, 576 (1975).
[4] J. Kim and R. C. Davis, Appl. Phys. Lett. 30, 130 (1977).
[5] A compilation of cross sections and rate coefficients for nonradiative processes involving hydrogen and its molecules is given in E. M. Jones, Culham Laboratory Report No. CLM-R 175, Culham Laboratory, Abingdon, England (unpublished). Similar data for ionization of H and H_2 are given in R. L. Freeman and E. M. Jones, Culham Laboratory Report No. CLM-R 137 (unpublished).
[6] M. Born and E. Wolf, *Principles of Optics,* 3rd ed. (Pergamon, London, 1965).
[7] D. H. McNeill and J. Kim, Oak Ridge National Laboratory Report No. ORNL/TM-7259 (unpublished).
[8] C. Karolis and E. Harting, J. Phys. B 11, 357 (1978).
[9] The factor 0.044 (k) in the denominator of the first part of Eq. (12) follows from the suggestion, based on $n=2$ and $n=4$ population measurements, in M. Vogler and G. H. Dunn, Phys. Rev. A 11, 1983 (1975), and R. A. Phaneuf, D. H. Crandall, and G. H. Dunn, Phys. Rev. A 11, 528 (1975), that about 10% of the atoms formed in dissociative recombination of H_2^+ are in the $n=3$ state (44% of these yield H_α).
[10] H. Kleinpoppen and E. Kraiss, Phys. Rev. Lett. 20, 361 (1968).
[11] L. Spitzer, *Physics of Fully Ionized Gases,* 2nd ed. (Wiley Interscience, New York, 1962).
[12] M. Misakian and J. C. Zorn, Phys. Rev. 6, 2180 (1972); S. R. Ryan, J. J. Spezeski, O. F. Kalman, W. E. Lamb, Jr., L. C. McIntyre, Jr., and W. H. Wing, Phys. Rev. A 19, 2192 (1979). Ryan *et al.*, report structure in the slow H(2s) group owing to predissociating vibrational levels that was obscured in the earlier work, apparently because of thermal motion of

the H_2 molecules. The H_α spectra calculated from the kinetic energy distributions of slow H(2s) given in these papers (see Fig. 3, curve B) are indistinguishable with the resolving power of our apparatus. Also, thermal motion will tend to smear out the predissociation peaks in the plasma.

[13]R. S. Freund, J. A. Schiavone, and D. F. Brader, J. Chem. Phys. 64, 1122 (1976).

[14]D. H. McNeill, Plasma Physics Laboratory, Princeton University Report No. PPPL-1758 (unpublished) and Bull. Am. Phys. Soc. 25, 877 (1980).

[15]H.S.W. Massey, in *Electronic and Ionic Impact Phenomena,* 2nd ed. edited by H. S. W. Massey, E. H. S. Burhop, and H. B. Gilbody (Oxford University Press, London, 1971),Vol. III.

[16]M. D. Gabovich, *Fizika i Tekhnika Plazmennykh Istochnikov Ionov* (The Physics and Engineering of Plasma Ion Sources) (Atomizdat, Moscow, 1972).

[17]For high filling pressures ($\gtrsim$3 mTorr), but not so high as to suppress the discharge, H_3^+ formation (reaction 4) is the dominant loss process for H_2^+ and $n_{H_2^+}$ is relatively independent of n_{H_2}; i.e., $n_{H_2^+}=\dot{n}_{H_2^+}\tau_{H_2^+}\approx n_e n_{H_2}\langle\sigma_{\rm ion}v_e\rangle/[n_{H_2}\langle\sigma_{H_3^+}v\rangle]$, so that $n_{H_2^+}\approx 8\times10^8 n_e\langle\sigma_{\rm ion}v_e\rangle$ (Ref. 5). This formula implies that $T_e\sim4$ eV for the typical measured $n_e=10^{12}$ cm^{-3} and $n_{H_2^+}=3\times10^{11}$ cm^{-3}. If, as probe data imply, T_e is usually somewhat lower in the discharge volume, then this relatively high value of $n_{H_2^+}$, derived from beam-species measurements, may be a result of fast electrons in the discharge volume or near the extraction electrodes.

[18]B. J. Wood and H. Wise, J. Phys. Chem. 65, 1976 (1961); J. Chem. Phys. 29, 1416 (1958).

[19]I. Ali-Khan, K. J. Dietz, F. Waelbroeck, and P. Weinhold, Report No. Jül-1597, Institut für Plasmaphysik der Kernforschungsanlage Jülich, Jülich, West Germany (unpublished).

[20]H. R. Griem, *Plasma Spectroscopy* (McGraw-Hill, New York, 1964).

[21]R. C. Williams, Phys. Rev. 54, 558 (1938).

[22]The FPI actually has an Airy function response (Ref. 6) but a Gaussian was used here for ease of calculation. The central fine-structure peak reported in Ref. 21 has a relative intensity of about 0.15, but here it has been enhanced to improve the fit between curves D and E. This difference from Ref. 21 and, especially, the apparent symmetry of curve A of Fig. 3 suggest differences in the excitation conditions and fine-structure intensities.

[23]See, for example, T. Ogawa and M. Higo, Chem. Phys. 52, 55 (1980), for data on H_β and references to other work.

[24]According to Ref. 19, γ for metals decreases with increasing atom energy over the range 0.1 eV $< E <$ 100 eV. Thus, because fast dissociation product atoms should undergo more wall reflections than slow atoms before they are lost and will lose energy during this time, the variation in γ with E may enhance the relative amount of fast ($E\sim3$ eV) compared to slow ($E\sim0.3$ eV) atoms in the discharge and cause the "re-excitation" atomic H_α profile to have a ">1 eV" component that is more intense than the "0.3 eV" component. Such a variation in γ may also partially explain the small amount of cold (0.025 eV) atoms seen in the conventional discharge, since atoms with $E<0.1$ eV have a much higher sticking probability than those with $E\sim0.3$ eV. On the other hand, since the measurements of Ref. 18 were presumably made with cold atoms (in equilibrium with the walls), it is doubtful that in our ion source γ comes as close to unity at low E as suggested in Ref. 19.

[25]Unexcited fast dissociation product atoms can be produced by electrons with $E_e>18$ eV and since, as we have seen, "atomic" H_α is significant, the actual energy of the responsible fast electrons may be substantially lower than the nominal 40 eV of Table I. However, a slight difference in the fast electron populations of the two duopigatron sources remains a plausible explanation of the differences in their H_α spectra. Note also that the two mechanisms proposed here for the fast atoms are related to the extent that ionization of H atoms is the origin of the H^+ ions in the plasma.

[26]D. H. McNeill, Bull. Am. Phys. Soc. 24, 971 (1979), and Plasma Physics Laboratory, Princeton University, Report No. PPPL-1625 (unpublished).